ELSEVIER

Journal of Photochemistry and Photobiology A: Chemistry 134 (2000) 37–44

Journal of Photochemistry and Photobiology A:Chemistry

www.elsevier.nl/locate/jphotochem

Photochemistry of valerophenone in solid solutions

Petr Klán [a,*], Jaroslav Janošek [a], Zdeněk Kříž [b]

[a] *Department of Organic Chemistry, Faculty of Science, Masaryk University, Kotlářská 2, 611 37 Brno, Czech Republic*

[b] *Laboratory of Biomolecular Structure and Dynamics, Faculty of Science, Masaryk University, Kotlářská 2, 611 37 Brno, Czech Republic*

Received 7 December 1999; received in revised form 14 February 2000; accepted 21 February 2000

Abstract

Photoreactivity of valerophenone was investigated in frozen solid solvents: benzene, cyclohexane, *t*-butanol, hexadecane, and water. Different product and mass distributions were followed during the course of the photoreaction. It was evidenced that a portion of ketone molecules is almost unreactive in the solid state due to physical restraints of the solid solvent cavity. Free rotation along the C–C bonds becomes difficult inside the cavity and it is probable that larger conformational changes are totally restricted. It was shown that a fraction of molecules having the favorable conformation for hydrogen abstraction reacts with the same photochemical efficiency no matter what solvent was used. The elimination/cyclization ratio of the Norrish Type II reaction was studied as a function of temperature. Variation of the ratios, characteristic for each solvent, diminished with decreasing temperature what has been rationalized in terms of the effective reaction cavity. The semi-empirical PM3 method and molecular mechanics MM3 force field calculations were performed to evaluate stabilities of the ground state valerophenone conformations.

Keywords: Photochemistry; Norrish Type II reaction; Valerophenone; Organized media; Effective reaction cavity; Solvent effects; Conformational search

1. Introduction

The photochemical cleavage and cyclization reaction of organic carbonyl compounds, especially aromatic alkyl ketones, possessing favorably oriented γ-hydrogens — Norrish Type II reaction — has been extensively studied over four decades [1–5]. However, in spite of enormous interest in the structure-reactivity aspects of this process, comparatively few reports describing γ-hydrogen abstraction reaction in the solid state have been published [6–8]. A typical representative of aromatic alkyl ketones, valerophenone, has been widely used as a UV actinometer in photochemical experiments [9–11]. This compound reacts on its alkyl chain via the triplet state to produce 1,4-biradical, which can cleave, cyclize, or disproportionate back to starting ketone depending on its conformation (Scheme 1) [1–5,12].

As known from earlier studies, alkyl phenyl ketone photoreaction kinetics and product distribution depends on several factors that relate to the triplet and biradical nature and interactions with the solvents [1–5,11,13–16]. It was shown that the kinetics and the product distribution may be altered significantly by solvent properties: (a) high dielectric and polar solvents affect the relative energies of the lowest lying n,π* and π,π* excited states, and (b) hydrogen-bonding solvents interact with 1,4-hydroxy biradical intermediates causing slowing down the disproportionation of the biradical intermediate to starting ketone.

There are many examples, which demonstrate how various types of constraining media influence the course of photoreactions of guest molecules [17,18]. Norrish Type II reaction of alkyl–aryl ketones has been studied on several derivatives in the solid state [19,20] as well as in various organized media. It is now well established that the biradical conformation and so the elimination–cyclization ratio is influenced by the type of the medium used: Dianin's compound [21], cyclodextrins [22], or zeolites [23–25]. Such media present surroundings, which prevent drastic conformational, translational, and rotational changes along the reaction coordinate [6–8,26,27].

We have recently studied valerophenone photoreactivity as part of our program on *microwave photochemistry* [28,29]. Now we wish to report on the photoreactivity of valerophenone in 'frozen' nonpolar as well as polar solvents. Such solid-state media offer an opportunity to study the well-known photoreactivity of valerophenone under conditions in which otherwise liquid ketone is more or

* Corresponding author.
E-mail address: klan@sci.muni.cz (P. Klán)

1010-6030/00/$ – see front matter
PII: S1010-6030(00)00244-6

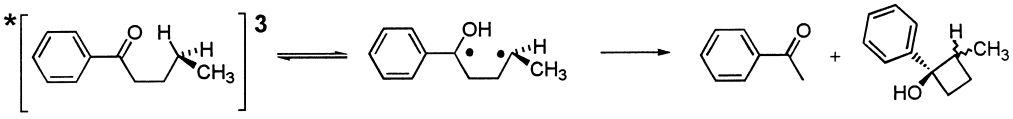

Scheme 1.

less constrained in a solvent cavity possessing a variety of electronic and steric properties.

2. Experimental

2.1. Equipment

Gas chromatography was accomplished on a Shimadzu GC-17A apparatus and on a GC/mass system TRIO 1000 (FISONS Instruments). Some compounds were analyzed by Kratos Kompact MALDI III. UV spectra were obtained on a Shimadzu UV-1601 instrument with matched 1.0 cm quartz cells. ^{1}H and ^{13}C NMR spectra were obtained for solutions in $CDCl_3$ on an Avance Bruker DRX 500. Low-temperature experiments were accomplished in the cryostat MLW MK70.

2.2. Chemicals and solvents

Valerophenone was obtained from Aldrich Chemical Co. and was purified by distillation under reduced pressure. Hexadecane (>99%) from Schuchardt was used as received. Reagent grade benzene was washed with sulfuric acid until further portions remained colorless, then washed with water, dried, and distilled over P_2O_5, bp 80°C. Reagent grade cyclohexane was worked up with sulfuric acid in the same way as benzene and then distilled over CaH_2, bp 81°C. Ethanol (analytical grade) was dried and distilled over sodium, bp 78°C. *t*-Butanol (analytical grade) from Merck was used as received. Hexane (analytical grade) from Park Scientific was dried and distilled over CaH_2, bp 69°C. Water was purified by the reverse osmosis process on an Aqua Osmotic 03 and its quality complied with US Pharmacopaial Standards (USP).

2.3. Irradiation procedures

All solutions were prepared directly by weighing the desired material into volumetric flasks or by dilution of stock solutions. Valerophenone solutions (10 ml) in 13 mm×100 mm Simax (Pyrex equivalent; >280 nm) tubes, sealed with a septum, were degassed by bubbling the solutions with argon for 15 min. Samples in a merry-go-round arrangement were placed into a cryostat box with ethanol as a cooling medium with temperature lowered to the desired value. Samples were irradiated using a 125 W medium-pressure mercury lamp (Teslamp).

Photochemical experiments in the liquid phase and the irradiation at −78°C (solid carbon dioxide bath) were accomplished using a conventional medium-pressure mercury lamp (125 W, Teslamp or 400 W, Conrad-Hanovia) with 2 mm thick Simax filter.

Photochemical efficiencies of the valerophenone reaction in frozen liquids were investigated in a quartz vessel which was made from a 13 mm×150 mm tube centered in a 35 mm×150 mm tube filled with the studied frozen solvent. The 10 ml of degassed 0.1 M valerophenone solution in the center tube, surrounded by the 10 mm layer of the solid material, was irradiated in a merry-go-round fashion by the 125 W Hg lamp at the desired temperature and wavelength, at the same time as valerophenone solution in the same vessel surrounded by ethanol. The irradiation was than repeated several times to get well reproducible results. The reproducibility was ±7% in all efficiency measurements.

2.4. Analysis of the irradiated samples

Photoproduct conversions, mass balance, and the elimination/cyclization ratios (*E*/*C*) were examined for every case as a function of time. The only photoproducts analyzed were acetophenone (**8**) and cyclobutanols (**7**). Formation of a minor photoproduct (<2% yield, assuming the same GC response factor as valerophenone) was also observed and was believed to be phenylcyclopentanol as described elsewere [11]. Identification of acetophenone, isolated by flash chromatography, and the remaining starting ketone in the sample was based on ^{1}H NMR, ^{13}C NMR, and on GC comparisons with authentic samples. Cyclobutanols were identified as described in the literature using GC and GC/mass instruments [11,29,30]. For comparison, a solution of 4×10^{-4} M valerophenone in acetone was irradiated using Simax-filtered radiation from Hg lamp until the reaction reached the first half-life. The products were analyzed by GC/mass spectrometry and the results were successfully compared to those described in the literature [11]. Concentrations of the photoproducts were calculated from peak integrations of data obtained with flame ionization detection, assuming that the cyclobutanols had the same response as valerophenone. The photoproducts were stable under GC conditions used. Each sample was analyzed three times; in case that the values differed by more than 5% the measurement was repeated. Samples were analyzed by GC with response factors for products, starting ketones, and hexadecane as internal standard.

Irradiated samples of approximately 10^{-3} M valerophenone in water were extracted with dichloromethane solution of hexadecane, as internal standard, and the solutions were GC analyzed. A non-soluble solid mass, formed during

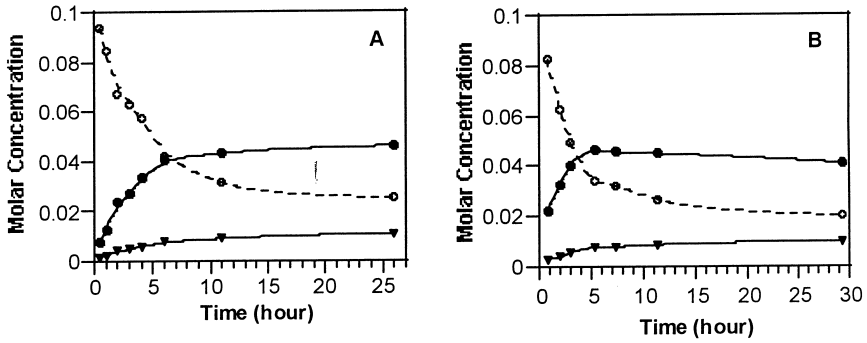

Fig. 1. Photolysis of the 0.1 M valerophenone solution (○: VP; dotted line): (A) in *t*-butanol/ethanol (9:1, v/v), and (B) in benzene at −20°C resulting in acetophenone and cyclobutanol formation (●, AP; ▼, CB; solid lines). The reproducibility of all measurements was ±5%.

some irradiation experiments, was isolated by filtration and analyzed on a MALDI instrument.

2.5. Conformational search

The conformational search was performed using the program VADER [31]. All energy calculations and minimizations were accomplished using semiempirical quantum chemistry program MOPAC-6.0 with PM3 method [32,33]. The same conformational search was made on the molecular mechanics energy calculation level using the program CICADA [34] and MM3 force field [35].

3. Results

Valerophenone photochemistry in 'frozen' solid solutions was studied in five different solvents: benzene, cyclohexane, *t*-butanol/ethanol (9:1, v/v) mixture, hexadecane, and water. The ketone solutions were quickly cooled to the desired temperature, at which the whole volume solidified, and irradiated at >280 nm by a 125 W mercury lamp. Decrease in valerophenone concentration as well as increase in acetophenone (**8**) and cyclobutanol (**7**) concentrations were followed in the course of the reaction by GC analyses.

Fig. 1A shows an example of valerophenone irradiation in a *t*-butanol/ethanol (9:1, v/v) mixture at −20°C. Time dependencies of the change in valerophenone (VP), acetophenone (AP), and cyclobutanol (CB) concentrations during the first several hours of irradiation were nearly linear. When irradiation continued the concentrations of all three analyzed compounds leveled off. There was a small but detectable continuing decrease in valerophenone and acetophenone concentrations after more than 24 h. Samples irradiated for a longer time contained a small amount of a yellowish solid (the mass balance from all experiments is discussed in the next chapter), which was analyzed by Kratos Kompact MALDI III. Those solids from experiments in various solvents were determined as a mixture of low-mass oligomers of valerophenone as well as acetophenone and a very small amount of unidentified high-mass polymers. Very similar valerophenone photochemical behavior was found in frozen benzene (Fig. 1B). Both the shape of the time-dependent concentration curves and the mass distribution were practically same.

The results from photochemical experiments in frozen cyclohexane and water (valerophenone concentration in water was approximately 0.001 M) were somewhat different (Fig. 2). In these solvents, concentration change characteristics resembled valerophenone photochemistry in benzene and *t*-butanol/ethanol mixture only during the first several hours. Valerophenone then continued to degrade and entirely vanished from the reaction mixture in about 40 h. However, both acetophenone and cyclobutanol concentra-

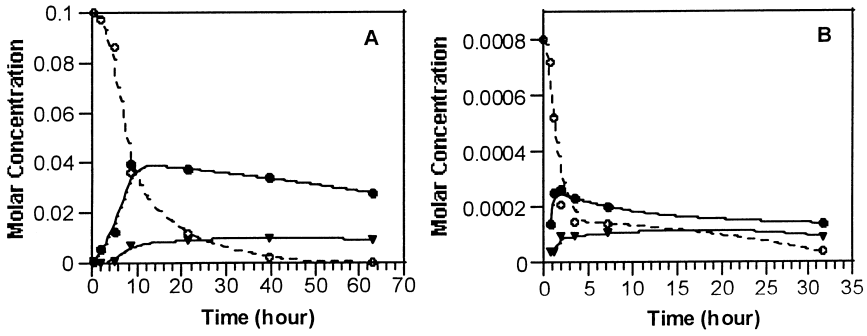

Fig. 2. Photolysis of the valerophenone solution (○: VP; dotted line): (A) in cyclohexane (0.1 M concentration), and (B) in water (ca. 0.001 M concentration) at −20°C resulting in acetophenone and cyclobutanol formation (●, AP; ▼, CB; solid lines). The reproducibility of all measurements was ±5%.

Table 1
Temperature dependent elimination/cyclization ratios (*E*/*C*)

Solvent	*E*/*C*[a]		
	20°C	−10°C	−30°C
t-BuOH–EtOH (9:1)	7.88±0.30 (9.00)[b] [36]	6.42±0.15	5.93±0.06
Benzene	4.52±0.11 (4.55) [36]	5.10±0.09	6.28±0.11
Cyclohexane	4.62±0.09	5.85±0.20	6.44±0.19
Hexadecane	4.84±0.12	5.44±0.07	5.68±0.19
Water	1.91±0.07 (2.03) [11]	2.74±0.05	3.62±0.14

[a] Values represent average of four measurements. The total mass balance never dropped below 95%.
[b] *t*-BuOH only.

tions remained at the plateau values again. At the same time, we observed the formation of higher-mass compounds in much larger amount than in two other solvents.

We also studied temperature dependencies of the Norrish Type II elimination/cyclization ratios in frozen solutions. Table 1 compares the values obtained in the liquid (20°C) as well as solid state.

We calculated the sum of the Boltzmann probabilities over all valerophenone (ground state) conformers. We have found 34 low energy conformers (local energy minima) and 139 conformational transition states by quantum mechanics calculations. The conformations were sorted into two families:

1. Favorable conformations (e.g., **2**, Scheme 2) where the values of the $C_\alpha-C_\beta$, $C_{CO}-C_\alpha$, and $C_\beta-C_\gamma$ torsions were in the intervals ⟨−90, 90⟩, ⟨−60, 60⟩, and ⟨120, 240⟩ degrees, respectively.
2. Unfavorable conformations (**1**, Scheme 2) where the values of the $C_\alpha-C_\beta$ torsion were in the intervals ⟨−180, −90⟩ and ⟨90, 180⟩ degrees and the $C_{CO}-C_\alpha$ and $C_\beta-C_\gamma$ torsions were complementary to those of favorable conformations.

Table 2 summarizes the values from the conformational search by both quantum mechanics as well as molecular mechanics calculations.

The results of the calculated Boltzmann probabilities as a function of the thermodynamic temperature are listed in Table 3. It was found that our molecular mechanics calculations were more sensitive to thermodynamic temperature than quantum mechanics calculations.

4. Discussion

Weiss et al. provided a model for the photobehavior of molecules in the constrained and organized media by characterization of the *effective reaction cavity* [26]. Some crystalline materials and zeolites, for instance, possess free volume that is essentially stationary and constant (*hard* cavities). On the other side, media such as micelles, microemulsions, and liquid crystals possess free volume, shape of which is changing in time (*soft* cavities). As *passive* was the reaction cavity described for cases when there are no

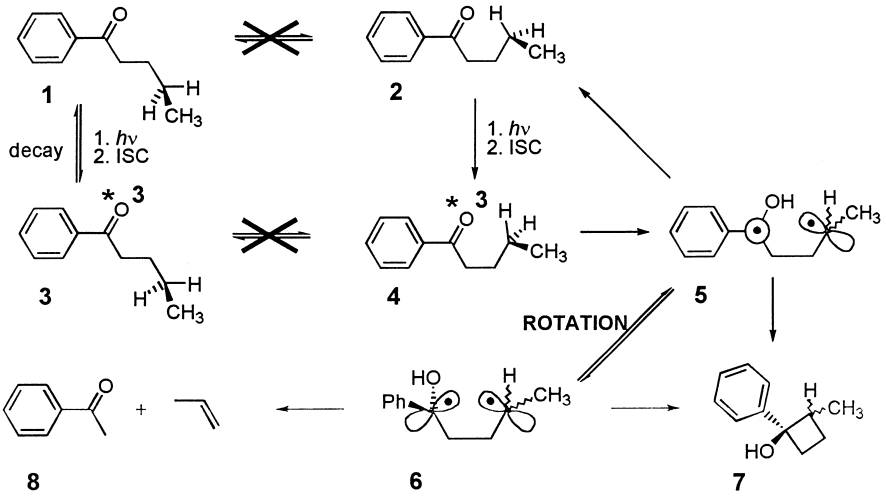

Scheme 2.

Table 2
Results of conformational search in valerophenone

Method used	Total number of conformations	Number of conformations		Sum of Boltzmann probabilities[a]	
		Favorable	Unfavorable	Favorable	Unfavorable
Quantum mechanics	34	22	12	39.5	60.5
Molecular mechanics	20	14	6	25.8	74.2

[a] The Boltzmann probabilities are calculated for the thermodynamic temperature 300 K.

Table 3
The change of the Boltzmann probabilities calculated for three different thermodynamic temperatures

Thermodynamic temperature (K)	Calculated Boltzmann probabilities of conformations (%)			
	Quantum mechanics		Molecular mechanics	
	Favorable	Unfavorable	Favorable	Unfavorable
300	39.5	60.5	25.8	74.2
250	36.9	63.1	17.8	82.2
200	33.9	66.1	9.3	90.7

interactions of a guest molecule with the cavity walls, while in the *active* cavity, interactions between the guest and host molecules cause their specific orientation. Thus, the photoreactivity of compounds inside the reaction cavity may vary upon the character of the organized medium. Here, we present results from the investigation of valerophenone photoreactivity in the solid matrices of 'frozen' solvents.

In Scheme 2, singlet excited valerophenone intersystem crosses effectively into the triplet state, which provides hydrogen abstraction following by the cyclization, elimination, or disproportionation reactions. As is apparent from the scheme, only a fraction of all valerophenone conformations (**4**) provide a favorable orientation for γ-hydrogen abstraction. The unfavorable conformer (**3**) may rotate into a favorable one within the excitation lifetime under unrestricted conditions. When such conformational motion is restricted the excited molecule decays.

4.1. Conformational restrictions and the product distribution

Results from our valerophenone irradiation in frozen solutions raise several questions. Fig. 1 shows a time-dependent change of starting valerophenone and photoproducts concentrations in non-polar benzene and a polar (hydrogen-bonding) *t*-butanol/ethanol (9:1, v/v) mixture at −20°C. Valerophenone light-induced consumption was almost linear during the first several hours and then the concentration decrease of the starting ketone, as well as the building up of the products, leveled off to a plateau. A fraction of 25–30% of molecules remained unreacted even after as long time as 30 h of irradiation. It is intriguing that the observed photochemical macroscopic behavior of valerophenone in those two frozen solvents was found to be almost identical despite of the fact that the character of both solvents and so the quality of solid-state cavities was different. Valerophenone molecules were partially constrained in the solid benzene in the same extent as in the *t*-butanol/ethanol mixture: the rotation along the C–C bonds became difficult and larger conformational changes were totally restricted (as illustrated in Scheme 2). In addition, we expect that diffusion of ketone molecules was entirely frozen in the solvent matrix. Thus, a nearly constant fraction (>70%) of valerophenone molecules were in reactive conformations or in conformations that could reach such favorable geometries within their excitation lifetime.

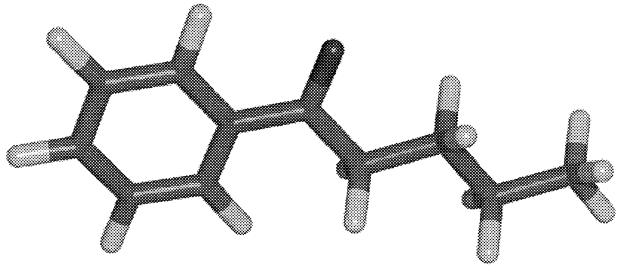

Fig. 3. Stretched (unfavorable) valerophenone conformation calculated by MM3.

It is now well established what are the geometrical requirements for intramolecular hydrogen transfer [2]. Although a linear O–H–C arrangement (the $C_\beta - C_\gamma$ torsion angle 180°) is preferred [37], it is known that hydrogen abstraction still occurs at values of the angle closer to 90° [38,39]. Our molecular mechanics calculations showed that 74–91% of valerophenone molecules, depending on temperature, are in the *unfavorable* conformation, which would preclude the hydrogen abstraction (Table 3). Somewhat lower values (60–66%) were found by quantum mechanics calculations, which were, however, not so much sensitive to the thermodynamic temperature change. In the MM3 force field calculations, the Boltzmann probabilities of low energy conformations increased when the thermodynamic temperature decreased. The drop was calculated as threefold when the temperature decreased by 100 degrees. This was expected because stretched conformations of flexible molecules are usually more populated at a lower temperature. Our calculated values, however, do not match our experimental results. This can be rationalize by the fact that the calculations show a ground-state-controlled static distribution [40–42] over all conformers without considering the time-dependent conformational change. A stretched unfavorable conformation is the most populated representative (Fig. 3; E_{rel}=0.0 kcal/mol [1]) while the ideal favorable *gauche* (Fig. 4; E_{rel}=2.9 kcal/mol; see Footnote 1) or the unfavorable anti-geometries (Fig. 5; E_{rel}=1.9 kcal/mol; see

[1] The relative energy obtained by MM3 force field calculations.

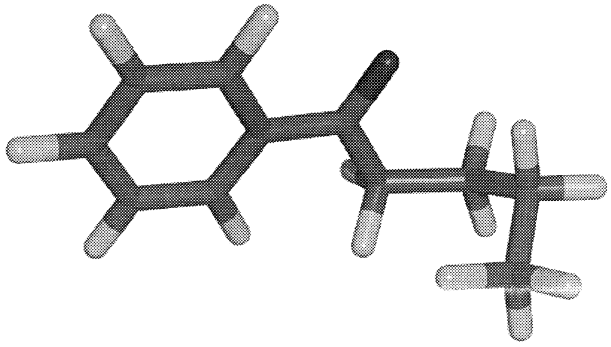

Fig. 4. *Gauche* (favorable) valerophenone conformation calculated by MM3.

Footnote 1) are populated more sparsely. It must be understood that the ∼10 ns lifetime of the excited valerophenone would allow only one or two twists along the C–C bonds when the molecule is unrestricted. Chandra and his coworkers [43] calculated conformational barriers to γ-hydrogen abstraction in several dialkyl ketones and they found that the major contribution to the reaction barrier comes from the rotation around the $C_\alpha-C_\beta$ bond in the lowest triplet state — the principal twist between the *gauche* or *anti* conformations. In the frozen cavity, such motion is expected to be even much less efficient. Our experiment showed that there is a fraction of specifically constrained (frozen) molecules (∼30%) thanks to the cavity size and/or intermolecular interactions between the ketone and solvent molecules as well as the temperature effect itself. Since calculations showed that 60–90% of molecules are in an unfavorable conformation, the difference (30–60%) should be attributed to the conformations, which are not in the favorable hydrogen abstraction geometry at the moment of the excitation but are allowed to rotate into one within the excitation lifetime.

It is evident that the reaction cavity is not entirely *hard* at temperatures when the medium is not completely solidified, which allows valerophenone to accomplish certain microscopic motions. This was confirmed by additional experiments at temperatures close to the melting point of the solvent. Here, the valerophenone photochemical degradation was, as expected, close to 100%. However, the product distribution in the temperature range from −10 to −30°C was found to be quite similar. On the other side, the irradiation of valerophenone solutions at −78°C was not very feasible because the conversion was very low (below 1% after 10 h of irradiation using 400 W lamp), obviously because of much *harder* restrictions in the environment and frozen conformational motion of valerophenone alkyl chain.

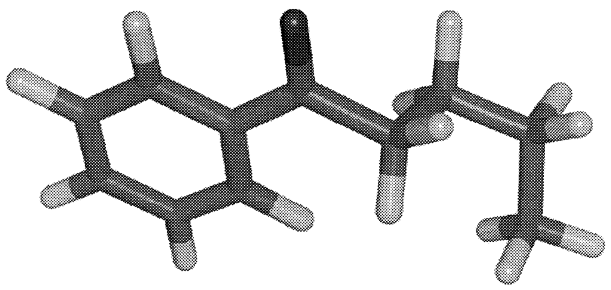

Fig. 5. *Anti* (unfavorable) valerophenone conformation calculated by MM3.

We could raise the question how the cavity size and shape or specific constraining interactions of host molecules with the guest influence valerophenone photochemistry in our experiments. Table 1 shows the elimination/cyclization (*E*/*C*) ratios in various solvents indicating that the *E*/*C* values regularly increased or decreased when going from 20 to −30°C; the tendency was characteristic for each solvent. The values were calculated for valerophenone conversions only when the total mass balance was higher than 95% to ascertain that valerophenone aggregation and so intermolecular reaction does not influence the ratio. The largest *E*/*C* change was observed in water that represents the most polar medium. Despite of the fact that the changes were not too dramatic in most presented cases, the tendencies were quite distinguishable. Changes in the *E*/*C* ratio values when temperature was lowered indicate that there are differences in the biradical conformational distribution (**5** ↔ **6**) thanks to either a lower temperature and/or ketone interactions with the solvent molecules of the cavity.

The Norrish Type II photoelimination and cyclization of phenyl alkyl ketones proceeds exclusively via intramolecular γ-hydrogen abstraction by an excited carbonyl group, producing a 1,4-biradical as a primary photoproduct (Fig. 6) [14]. Further reactions are dependent on the biradical conformation. When the p-orbitals of the radical centers can overlap (in *cisoid* or *gauche* conformations), cyclobutanol is formed (usually 5–10% in liquid solutions). When the p-orbitals of the radical centers are parallel to the $C_\beta-C_\gamma$ bond (*gauche* or *anti* conformations), the bond will cleave to give an enol and an alkene (25–40%) or the disproportionation gives the starting ketone (50–70%) [2]. When hydrogen abstraction occurs the triplet biradical must intersystem cross to the singlet biradical to provide singlet products. It is unlikely that an *anti* (e.g. stretched) biradical conformation is ever reached in the frozen solvent cavity because it requires a dramatic conformational change. Thus, *cisoid* and *gauche* conformations are the only likely sources of the photoproduct formation and so most of the cleavage occurs from the *gauche* biradical. Scaiano has postulated that triplet biradical decay is determined by rates of intersystem crossing (ISC): the Norrish Type II product distribution depends on the biradical conformation at

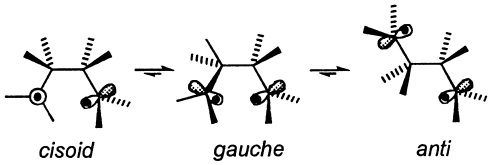

Fig. 6. Product formation based on the 1,4-biradical geometry [2].

the moment of ISC [16,44]. He found that when the radical sites are farther apart the biradical lifetimes are much longer. Thus, we expect that the biradical in the frozen cavity, having only *gauche* or *cisoid* conformations, facilitates faster ISC than that in solution. In case that *anti* biradical conformations are abandoned one would also expect a decrease in the *E*/*C* ratio with decreasing temperature since those conformations provide only elimination reaction. It was, however, observed only in the frozen *t*-butanol/ethanol mixture (Table 1). Furthermore, the *E*/*C* ratios at −20°C seem to be nearly identical in all types of solvent used: the differences in *E*/*C* values for different solvents disappear when temperature drops. This might be explained by very similar conformational distribution of the molecule in all matrixes and be another evidence that *hardness* of the cavity in the solid solutions increases going from −10 to −30°C.

4.2. Molecular aggregation

Fig. 2 compares valerophenone photochemistry in frozen cyclohexane (0.1 M solution) and in water (ca. 0.001 M solution). Here, valerophenone entirely vanished from the solid solutions in ∼40 h unlike to the experiments in frozen benzene and *t*-butanol mixture; the photoproduct concentrations, however, leveled off similarly. Valerophenone concentration slowly dropped in the course of the reaction along with simultaneous formation of high-mass compounds (especially dimers and oligomers of valerophenone), caused by valerophenone aggregation in the frozen solvent (evidently the largest in water and cyclohexane), and resulting in intermolecular reactions such as photoreduction. The mass balance after 24 h of irradiation is shown in Table 4. Aggregation obviously depended on ketone solubility in solvents and the ability to aggregate during the process of solidification.

4.3. Photochemical efficiency

Kinetic analysis of valerophenone photoreaction in the liquid solution that have been conducted under optically opaque conditions with low conversions to photoproducts provided usually zero-order plots with respect to ketone concentration and the reaction was proportional to the quantum yield. Linear pseudo-first-order plots up to ∼90% conversion were observed in aqueous media where, thanks to a low valerophenone solubility, only a small fraction of the incident light is absorbed [11,45].

Table 4
The mass balances during valerophenone photoreaction in frozen solutions after 24 h of irradiation at −20°C

Solvent	[VP] (%)[a]	[AP] (%)[a]	[CB] (%)[a]
Benzene	24	45	10
t-Butanol	25	43	9
Cyclohexane	11	38	9
Water	9	20	7

[a] The reproducibility of all measurements was ±8%.

We carried out the simultaneous experiments of valerophenone photodegradation in three frozen solvents and liquid hexane at −20°C. A plot of acetophenone formation dependence on time during the first several hours provided nearly linear dependencies with the same slope for frozen benzene, cyclohexane, and *t*-butanol/ethanol mixture (Fig. 7). It means that a fraction of molecules having the favorable conformation for hydrogen abstraction reacts with the same photochemical efficiency no matter what solvent was used.

It is well known that quantum yields of the Type II reaction of valerophenone in benzene and alkanes at 313 nm are in the range of 0.3–0.4 [9,36]. On the other side, quantum yields are known to rise to unity in acetonitrile, ethanol, and water; thus an increase by a factor of 3. It is explained by formation of the hydrogen bond between the OH group of the biradical and the solvent what slows down the disproportionation, thus increase the quantum efficiency. We found equal quantum efficiencies in all (protic and non-protic) frozen solvents. This suggests that there are no significant interactions of solvent molecules with the biradical OH group in the reaction cavity. Such cavities could be described as

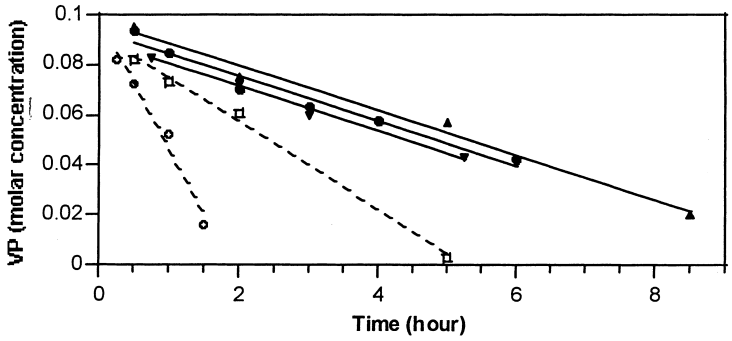

Fig. 7. Effects of solvent type and temperature on valerophenone photodegradation. Valerophenone concentrations in frozen solvents (−20°C; solid lines): (●), benzene; (▲), cyclohexane; (▼), *t*-butanol/ethanol (9:1, v/v), and in liquid solutions: (□), hexane (−20°C; dotted line); (○): benzene (20°C; dotted line). The reproducibility of all measurements was ±5%.

passive cavities. Valerophenone in cold hexane and in 20°C benzene solutions degraded faster than that in frozen matrix.

Furthermore, quantum efficiency of the photoreaction in liquid solutions is higher obviously due to light scattering, reflection, and a different absorption by the solid material. We tried to estimate the lowering the reaction efficiency thanks to those effects in the frozen matrix. A 10 mm coat of the frozen solvent around the tested valerophenone solution caused approximately 11–48% decrease in acetophenone formation depending on the type of the solvent used when irradiated at >280 nm [46]. This number in a good accord with the efficiency comparison in the solid and liquid state presented in Fig. 7.

Acknowledgements

This work was supported by grant CEZ: J07/98:143100005 of the Czech Ministry of Education, Youth and Sport. We thank L. Baráková for some photochemical efficiency measurements.

References

[1] P.J. Wagner, Acc. Chem. Res. 4 (1971) 168.
[2] P.J. Wagner, B.-S. Park, Photoinduced hydrogen atom abstraction by carbonyl compounds, in: A. Padwa (Ed.), Org. Photochem. 11 (1991) 227 and references therein.
[3] P.J. Wagner, G.S. Hammond, J. Am. Chem. Soc. 88 (1966) 1245.
[4] P.J. Wagner, Acc. Chem. Res. 16 (1983) 461.
[5] M.B. Zimmt, C.E. Doubleday Jr., N.J. Turro, Chem. Phys. Lett. 134 (1987) 549.
[6] S. Ariel, V. Ramamurthy, J. R Scheffer, J. Trotter, J. Am. Chem. Soc. 105 (1983) 6959.
[7] S. Evans, N. Omkaram, J.R. Scheffer, J. Trotter, Tetrahedron Lett. 26 (1985) 5903.
[8] V. Ramamurthy, K. Venkatesan, Chem. Rev. 87 (1987) 433 and references therein.
[9] P.J. Wagner, A.E. Kemppainen, H.N. Schott, J. Am. Chem. Soc. 95 (1973) 5604.
[10] R.A. Caldwell, S.N. Dhawan, T. Majima, J. Am. Chem. Soc. 106 (1984) 7480.
[11] R.G. Zepp, M.M. Gumz, W.L. Miller, H. Gao, J. Phys. Chem. A 102 (1998) 5716 and references therein.
[12] R.G.P.J. Wagner, Acc. Chem. Res. 22 (1989) 83.
[13] P.J. Wagner, Acc. Chem. Res. 22 (1989) 83.
[14] P.J. Wagner, P.A. Kelso, A.E. Kemppainen, J.M. McGrath, H.N. Schott, R.G. Zepp, J. Am. Chem. Soc. 94 (1972) 7506.
[15] P.J. Wagner, A.E. Kemppainen, H.N. Schott, J. Am. Chem. Soc. 95 (1973) 5604.
[16] J.C. Scaiano, Acc. Chem. Res. 15 (1982) 252.
[17] K. Kalyanasundram, Photochemistry in Microheterogenous Systems, Academic Press, New York, 1987.
[18] V. Ramamurthy, Photochemistry in Organized and Constrained Media, VCH, New York, 1991.
[19] S. Ariel, V. Ramamurthy, J.R. Scheffer, J. Trotter, J. Am. Chem. Soc. 105 (1983) 6959.
[20] S. Evans, N. Omkaram, J.R. Scheffer, Tetrahedron Lett. 26 (1985) 5903.
[21] P.G. Goswami, P. de Mayo, N. Ramnath, G. Bernard, N. Omkaram, J.R. Scheffer, Y.F. Wong, Can. J. Chem. 63 (1986) 2719.
[22] S. Sharat, G. Usha, C.H. Tung, N.J. Turro, V. Ramamurthy, J. Org. Chem. 51 (1986) 941.
[23] N.J. Turro, P. Wan, Tetrahedron Lett. 25 (1984) 3655.
[24] V. Ramamurthy, D.R. Corbin, D.F. Eaton, N.J. Turro, Tetrahedron Lett. 30 (1989) 5833.
[25] V. Ramamurthy, D.R. Corbin, D.F. Eaton, J. Org. Chem. 55 (1990) 5269.
[26] R.G. Weiss, V. Ramamurthy, G.S. Hammond, Acc. Chem. Res. 26 (1993) 530.
[27] M.D. Cohen, Angew. Chem., Int. Ed. Engl. 14 (1975) 386.
[28] P. Klán, J. Literák, M. Hájek, J. Photochem. Photobiol. A: Chem. 128 (1999) 145.
[29] P. Klán, J. Literák, Collect. Czech. Chem. Commun. 64 (1999) 2007.
[30] R.B. LaCount, C.E. Griffin, Tetrahedron Lett. 21 (1965) 1549.
[31] M. Černohorský, S. Kettou, J. Koča, J. Chem. Nf. Omput. Sci. 39 (1999) 705.
[32] J.J. Steward, J. Comput. Chem. 10 (1989) 209.
[33] J.J. Steward, J. Comput. Chem. 10 (1989) 221.
[34] J. Koča, P.H. Carlsen, J. Mol. Struct. (Theochem.) 308 (1994) 13.
[35] MM3 (92), Creative Arts Building 181, Indiana University, Bloomington, IN 47405, QCPE.
[36] P.J. Wagner, J. Am. Chem. Soc. 89 (1967) 5898.
[37] A.E. Dorigo, K.N. Houk, J. Am. Chem. Soc. 109 (1987) 2195.
[38] P.J. Wagner, P.A. Kelso, A.E. Kemppainen, R.G. Zepp, J. Am. Chem. Soc. 94 (1972) 7500.
[39] J.R. Scheffer, Org. Photochem. 8 (1987) 249.
[40] P.J. Wagner, P. Klán, J. Am. Chem. Soc. 121 (1999) 9635.
[41] M.A. Winnik, Chem. Rev. 81 (1981) 491.
[42] P.J. Wagner, Acc. Chem. Res. 16 (1983) 461.
[43] D. Sengupta, R. Sumathi, A.K. Chandra, J. Photochem. Photobiol. A: Chem. 60 (1991) 149.
[44] J.C. Scaiano, Tetrahedron 38 (1982) 819.
[45] R.G. Zepp, Environ. Sci. Technol. 12 (1978) 327.
[46] L. Baráková, unpublished results.